1 Introduction

This report presents a study of epidemic spreading dynamics in complex networks using the Susceptible-Infected-Susceptible (SIS) model. In this model, each node represents an individual who can be in one of two states: Susceptible (healthy but can get infected) or Infected (has the disease and can spread it to neighbors). Unlike the SIR model, recovered individuals in the SIS model become susceptible again, making it suitable for modeling diseases that do not confer long-term immunity.

We investigate how the fraction of infected nodes (ρ) in the stationary state varies with the probability of infection (λ) for different probability of recovery (μ) and network topologies. We compare the epidemic spreading behavior between Erds-Rényi (ER) random networks and Barabási-Albert (BA) scale-free networks and validate our Monte Carlo simulation results against theoretical predictions from the Microscopic Markov Chain Approach (MMCA).

2 Methodology

2.1 Network Models

We generated four different network topologies, each with 1000 nodes:

- Erdős-Rényi (ER) with average degree $\langle k \rangle = 4$, which we will refer to as ER_4 throughout this document
- Erdős-Rényi (ER) with average degree $\langle k \rangle = 6$, which we will refer to as ER_6
- Barabási-Albert (BA) with average degree $\langle k \rangle = 4$, which we will refer to as BA_4
- Barabási-Albert (BA) with average degree $\langle k \rangle = 6$, which we will refer to as BA_6

2.2 Monte Carlo Simulations

We implemented a discrete-time stochastic simulation of the SIS model on networks. The algorithm works as follows:

1. Initialize the network with 50 randomly infected nodes
2. At each time step:
   - Infected nodes recover with probability μ
   - Susceptible nodes become infected with probability $1 - (1 - \lambda)^{n_I}$, where n_I is the number of infected neighbors
   - Update all states simultaneously
3. Run the simulation until the system reaches a stationary state
4. Record the fraction of infected nodes ρ at steady state

We ran simulations for infection probabilities ranging from $\lambda = 0$ to $\lambda = 0.3$ (with $\Delta\lambda = 0.01$) and for two recovery probabilities: $\mu = 0.2$ and $\mu = 0.4$. For each parameter combination, we performed 600 realizations with different random seeds to calculate mean values and standard deviations.

2.3 Theoretical Approach: MMCA

To validate our Monte Carlo results, we implemented the Microscopic Markov Chain Approach (MMCA), which provides a theoretical prediction of the steady-state behavior. The MMCA models the probability of each node being infected over time through a set of coupled discrete-time equations:

$$\rho_i^I(t+1) = (1-\mu)\rho_i^I(t) + \rho_i^S(t)q_i(t) \tag{1}$$

where $\rho_i^I(t)$ is the probability that node i is infected at time t, $\rho_i^S(t) = 1 - \rho_i^I(t)$ is the probability of being susceptible, and $q_i(t)$ is the probability of node i becoming infected by its neighbors:

$$q_i(t) = 1 - \prod_{j=1}^{N}(1 - \lambda A_{ij}\rho_j^I(t)) \tag{2}$$

where A_{ij} is the adjacency matrix of the network.

2.4 Theoretical Epidemic Threshold Calculation

For each network considered in this study, we compute the theoretical epidemic threshold λ_c according to the relation:

$$\lambda_c = \frac{\mu}{\Lambda_1}$$

where Λ_1 is the largest eigenvalue of the network's adjacency matrix. This spectral threshold serves as a key reference to understand the onset of epidemic spreading in different network topologies.

The computed values are summarized in Table 1.

μ	BA_4	BA_6	ER_4	ER_6
0.2	0.0198	0.0146	0.0386	0.0283
0.4	0.0395	0.0293	0.0771	0.0566

Table 1: Theoretical epidemic thresholds computed as $\lambda_c = \mu/\Lambda_1$ for each network and recovery probability.

3 Results and Discussion

3.1 Steady-State Behavior

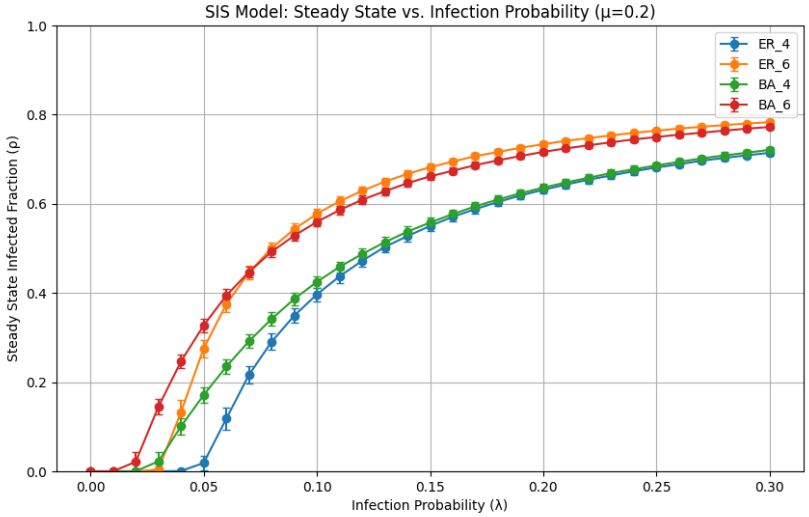

Figure 1: Steady-state infected fraction (ρ) as a function of infection probability (λ) for different network topologies with $\mu = 0.2$. Error bars represent standard deviation across 600 independent realizations.

Looking at Figure 1, we can make several important observations. First, the BA networks (green and red curves) start showing infections at much lower λ values than the ER networks (blue and orange curves) with the same average degree. For example, the BA_6 network (red) becomes infected around $\lambda \approx 0.02$, while the ER_4 network (blue) requires $\lambda \approx 0.05$ for a comparable onset. This behavior is consistent with the theoretical thresholds shown in Table 1.

Second, networks with higher average degree experience epidemics at lower infection probabilities and reach higher steady-state infection levels. Comparing ER_6 to ER_4, and BA_6 to BA_4, clearly shows that more connected networks facilitate disease spread.

Third, at moderate to high infection probabilities (λ between 0.10 and 0.30), the differences between BA and ER networks with the same average degree become less pronounced. This suggests that while network structure heavily influences the epidemic threshold, the average number of connections plays a dominant role in determining the final steady-state infected fraction once the epidemic is well established.

Finally, the earlier epidemic onset observed in BA networks can be attributed to the presence of highly connected hubs, which act as efficient spreaders and lower the effective threshold. The network heterogeneity, reflected in the degree distribution, accelerates the spread compared to the more homogeneous ER networks. Furthermore, the smaller error bars observed for BA networks indicate more consistent spreading dynamics across simulations, as the hubs dominate the transmission process and reduce variability.

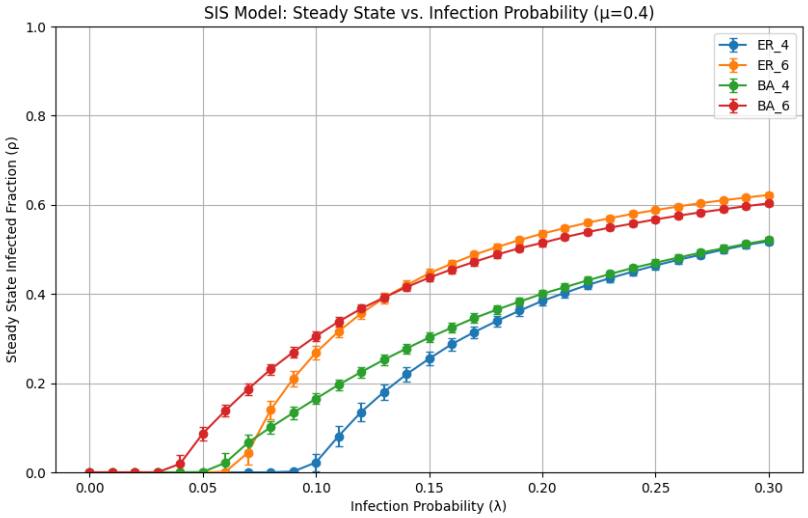

Figure 2: Steady-state infected fraction (ρ) as a function of infection probability (λ) for different network topologies with $\mu = 0.4$. Error bars represent standard deviation across 50 independent realizations.

Figure 2 shows the same relationship but with a higher recovery probability of $\mu = 0.4$. As expected, when infected nodes recover more quickly, the disease has a harder time spreading through the network. We can see that the epidemic thresholds have shifted to the right (higher λ values) compared to Figure 1, and the overall infected fractions are lower across all networks.

The same patterns we observed with $\mu = 0.2$ still hold: BA networks have lower thresholds than ER networks, and networks with higher average degree (ER_6 and BA_6) show more extensive spreading than those with lower degree (ER_4 and BA_4). However, the gap between the different network types is more pronounced with this faster recovery rate, showing that network structure becomes even more important when the disease is less aggressive.

The maximum infection levels reached at $\lambda = 0.3$ are now only about 60% for the higher-degree networks, compared to nearly 80% when $\mu = 0.2$, demonstrating how a faster recovery rate can significantly reduce the overall impact of an epidemic.

3.2 Effect of Network Topology and Recovery Rate

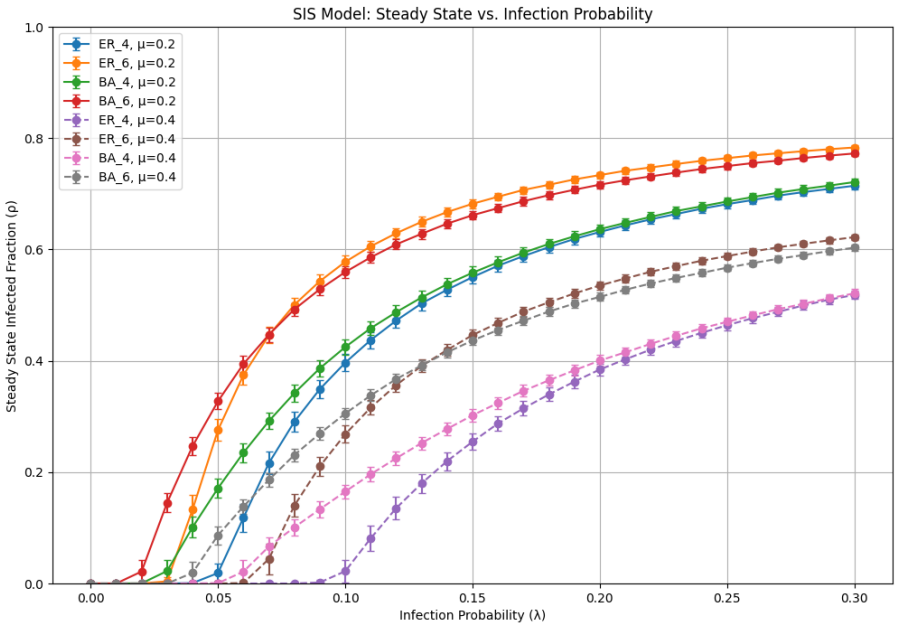

Figure 3: Comparison of steady-state infected fraction (ρ) across all network types and recovery rates. Solid lines represent results for $\mu = 0.2$, while dashed lines represent $\mu = 0.4$. Error bars show standard deviation across 600 independent realizations.

Figure 3 presents a comprehensive view of our results, allowing us to examine the combined effects of network structure and recovery rate on epidemic spreading. While we've already discussed many of the individual patterns in previous sections, this combined visualization reveals additional insights.

The most notable new observation is the **impact of recovery rate across different network types**. When we double the recovery rate from $\mu = 0.2$ to $\mu = 0.4$, all curves shift to the right and downward - meaning the disease needs to be more contagious to spread, and fewer people get infected overall. Interestingly, this effect is stronger in ER networks than in BA networks, suggesting that scale-free networks are harder to protect just by increasing recovery rate.

This finding has important practical implications: in populations with scale-free contact patterns (like many real-world social networks), strategies focused only on increasing recovery rates (through better treatment, for example) may be less effective than expected. For such networks, targeting the highly-connected hubs through vaccination or isolation might prove more effective.

The combined view reinforces our understanding that both recovery dynamics and network structure significantly influence epidemic outcomes, and strategies for disease containment should account for the underlying connectivity patterns of the population.

3.3 Comparison with Theoretical Predictions

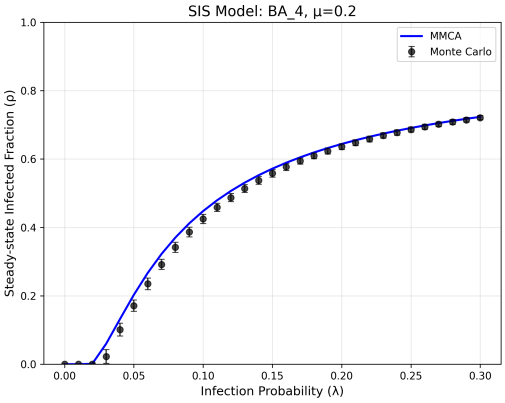

(a) BA_4 network, $\mu = 0.2$

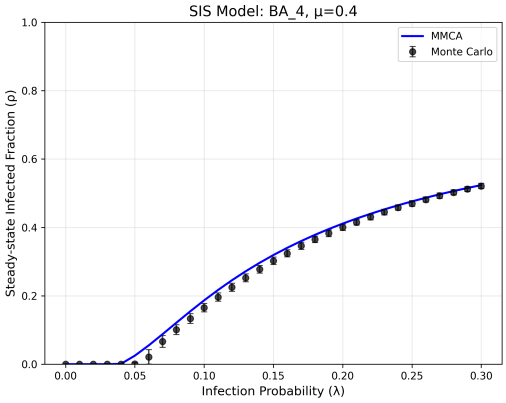

(b) BA_4 network, $\mu = 0.4$

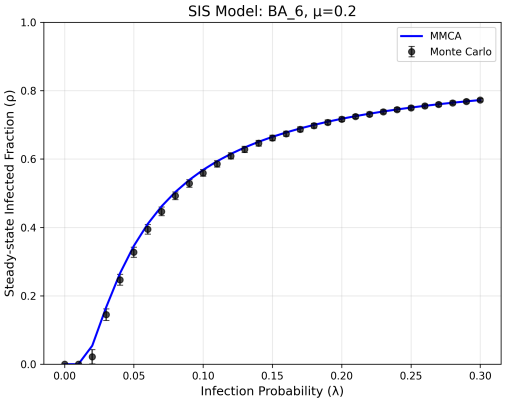

(c) BA_6 network, $\mu = 0.2$

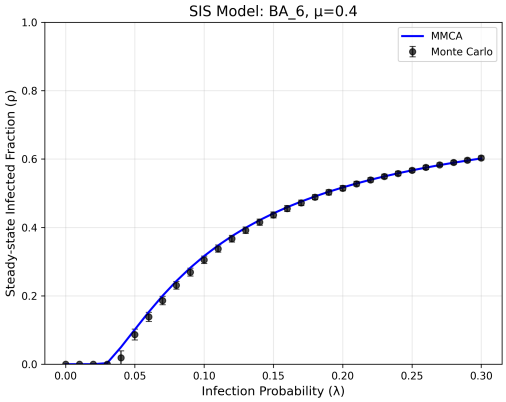

(d) BA_6 network, $\mu = 0.4$

Figure 4: Comparison between Monte Carlo simulations and MMCA theoretical predictions for BA networks.

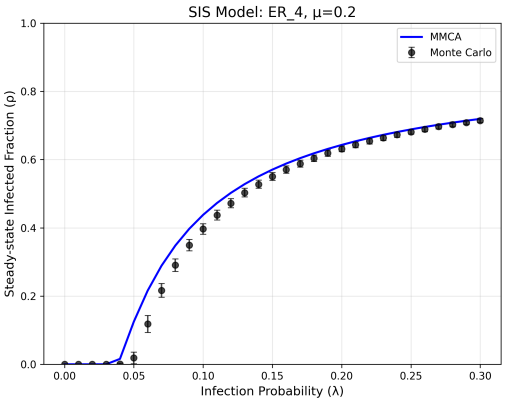

(a) ER_4 network, $\mu = 0.2$

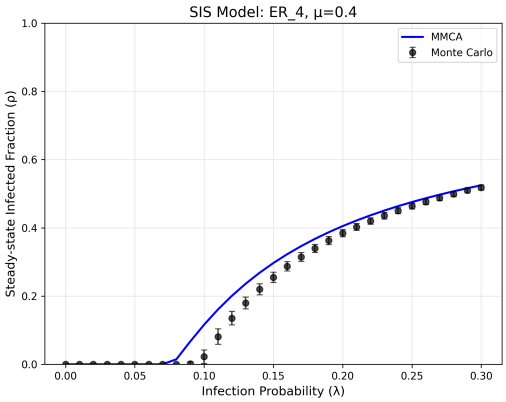

(b) ER_4 network, $\mu = 0.4$

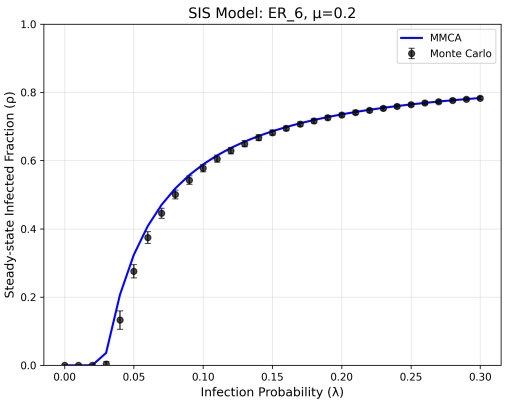

(c) ER_6 network, $\mu = 0.2$

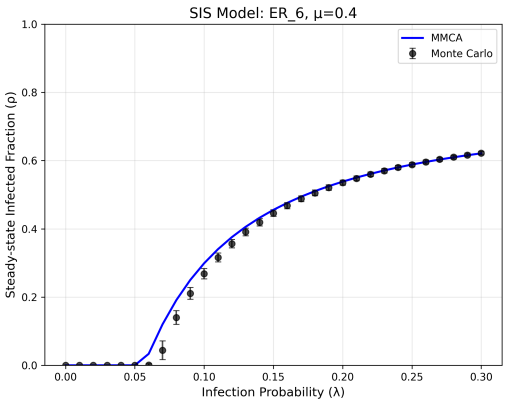

(d) ER_6 network, $\mu = 0.4$

Figure 5: Comparison between Monte Carlo simulations and MMCA theoretical predictions for ER networks.

Figures 4 and 5 compare our Monte Carlo simulation results with the theoretical predictions from the MMCA model. The solid blue lines represent the MMCA theoretical predictions, while the black dots with error bars show the results from multiple Monte Carlo simulation runs.

Looking at these comparisons, we can see that the MMCA approach provides remarkably accurate predictions across most scenarios. The BA networks (particularly BA_4 and BA_6 with $\mu = 0.2$) show especially good agreement between theory and simulation. For these scale-free networks, both the predicted epidemic threshold and the steady-state infection levels closely match the stochastic simulation results.

For ER networks, we observe slightly more noticeable discrepancies, especially near the epidemic threshold. In Figures 5a and 5c, the MMCA model predicts a somewhat sharper transition than what we see in the Monte Carlo simulations. This difference is most visible in the range between $\lambda = 0.05$ and $\lambda = 0.1$ for ER networks.

Some discrepancies between simulation and theory can be attributed to:

- Stochastic fluctuations in the Monte Carlo simulations, especially near the epidemic threshold where the system is most sensitive to random events
- Our simulations use networks with 1000 nodes, which is a practical size for our study. Theoretical approaches often work best when applied to extremely large networks. With our moderately sized networks, the transitions between disease-free and epidemic states appear more gradual than the sharp transitions that theory might predict.
- The MMCA method makes certain simplifying assumptions about how the disease spreads through the network. These simplifications work well in most cases, but they seem less accurate near the

point where the disease is just beginning to spread. In this critical region, the actual simulation results show more variability than the smoother theoretical predictions.

Despite these minor differences, our results show that MMCA predictions generally match well with the Monte Carlo simulations. This good agreement suggests that both approaches capture the fundamental aspects of how diseases spread through networks. The MMCA approach offers a significant practical advantage: it is much faster to calculate compared to running many Monte Carlo simulations. This suggests that both methods could be used together in future studies. Monte Carlo for the most accurate results in critical regions, and MMCA for quick estimations and exploration of many different scenarios.

4 Conclusion

Our study confirms that network topology significantly influences epidemic spreading dynamics in the SIS model. The heterogeneous degree distribution of BA networks leads to different epidemic behavior compared to more homogeneous ER networks, particularly in terms of the epidemic threshold and the relationship between infection probability and steady-state prevalence.

The comparison between Monte Carlo simulations and MMCA theoretical predictions demonstrates that the MMCA approach provides a reliable approximation of epidemic-spreading dynamics on networks, offering a computationally efficient alternative to extensive stochastic simulations.

Through this project, we have gained valuable insight into how diseases spread across different network structures. We were particularly surprised by how dramatically the presence of hub nodes in BA networks lowers the epidemic threshold, meaning diseases can start spreading even when they are not very contagious. This helped us understand why targeting highly-connected individuals (like through vaccination) could be so effective in real-world epidemic control

Working with both theoretical and simulation approaches taught us that each has its strengths – Monte Carlo simulations capture the randomness inherent in real-world disease spread, while the MMCA provides a faster "big picture" view. The strong agreement between these methods reinforced our confidence in the results.

If we were to extend this project, we would be interested in exploring more complex network models that better represent real social structures, or investigating adaptive networks where connections change in response to the epidemic. We believe these findings have important implications for understanding and controlling disease spread in real-world networks, which often exhibit scale-free properties similar to the BA model.

5 Appendix: Implementation Details

The simulations were implemented in Python, utilizing the NetworkX library for network generation and analysis. All code was executed within Jupyter Notebook environments. For the Monte Carlo simulations, we performed multiple sequential realizations to collect statistical data. These simulations were vectorized using NumPy to improve computational efficiency.

Simulation results were stored in CSV format to facilitate subsequent analysis and visualization. Plots were generated with Matplotlib, and statistical analyses were conducted using NumPy and Pandas.

The source code, network data, and result files are included in the submission package to ensure full reproducibility.